Rational Design Of Helical Peptoids For Tetracycline Conjugation: Insights Into Molecular Complexation Mechanisms

Andra Mihaela Onaș[1], Louis Groignet[2], Sorin Marius Avramescu[3], Horia Iovu[1,4]* and Julien De Winter[2]*

[1]Advanced Polymer Materials Group, National University of Science and Technology Politehnica Bucharest, 1-7 Gheorghe Polizu, Sector 1, 011061 Bucharest, ROMANIA
[2]Laboratory of Organic synthesis and mass spectrometry (S²MOs), Université de Mons, 23 Place du Parc, 7000 Mons, BELGIUM
[3]Faculty of Animal Productions Engineering and Management, University of Agronomic Sciences and Veterinary Medicine of Bucharest, 59 Marasti Bvd., Sector 1, 011464 Bucharest, ROMANIA
[4]Academy of Romanian Scientists, Ilfov 3, 050044 Bucharest, Romania

Abstract

This work addresses the need for cost-effective, stable, and sensitive detection of tetracycline, which is a widely used antibiotic molecule, with environmental and health risks associated with incorrect use. We have explored the use of N-substituted polyglycine oligomers (peptoids) as molecules capable of tetracycline conjugation. Peptoids are readily synthesized by solid-phase synthesis, offering great chemical diversity and enhanced stability. Inspired from a short aptamer which selectively binds tetracycline, we designed helical peptoids containing sidechains selected for their ability to promote π-π stacking interactions and hydrogen bonding. Five peptoid sequences were selected, differing in monomer order, and their complexation capacity was investigated using different mass spectrometric techniques and circular dichroism. Tandem mass spectrometry and ion mobility spectrometry investigation confirmed complex formation between peptoids and tetracycline. Additionally, circular dichroism revealed that the peptoid sequence influences the complexation. Our findings demonstrate the potential for rationally designed peptoids which can be used as capture probes for sensing applications.

Keywords: Peptoids, tetracycline, molecular complexation, mass spectrometry, circular dichroism

*Corresponding authors: Julien.dewinter@umons.ac.be & horia.iovu@upb.ro

Graphical Abstract

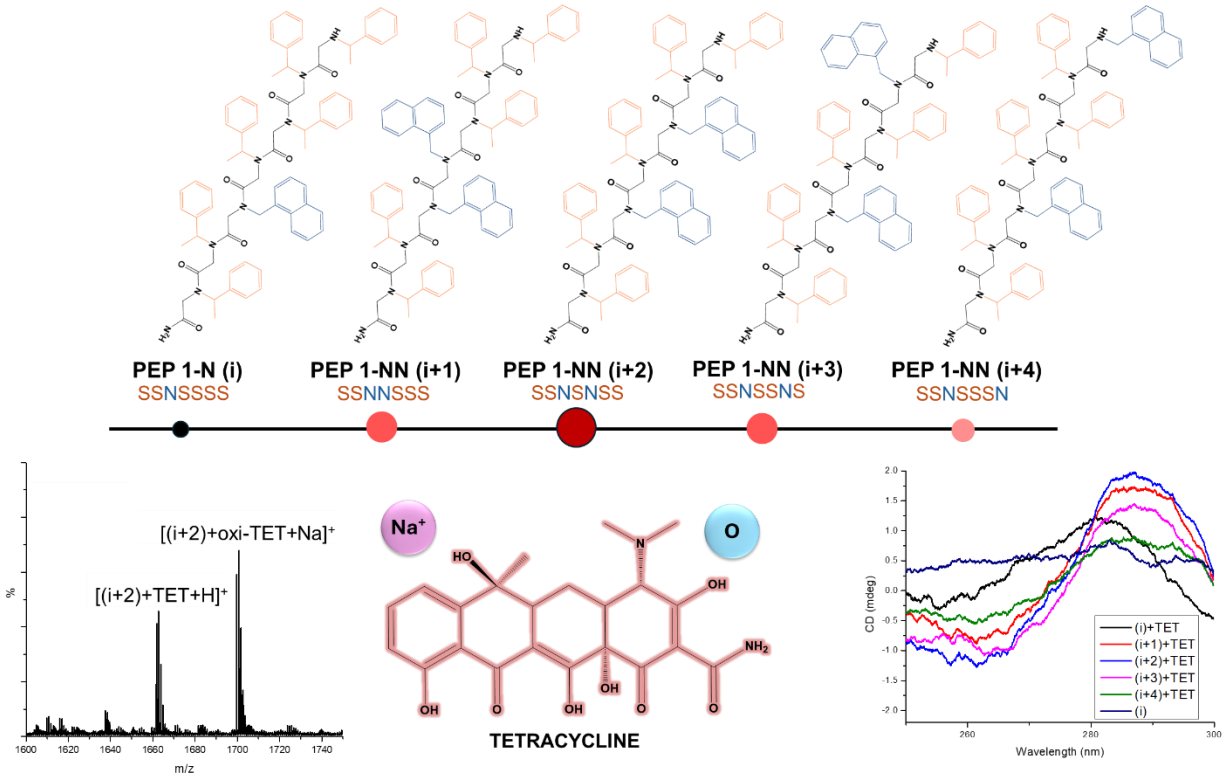

Introduction

Tetracycline is among the most often used broad-spectrum antibiotics and has been widely prescribed for both human and veterinary uses since its first report in the 1940s[1]. It is often used to treat various types of infections through its bacterial protein synthesis inhibiting activity. Extensive antibiotic utilization presents a high environmental and food safety risk, necessitating good monitoring and control. Moreover, antibiotic contamination poses a great problem for the increasing antibiotic resistance. The primary purpose of antibiotic sensing is therefore to allow precise measurement of trace levels in various matrices like food and feedstock, surface water or soil, in order to limit the overuse adverse effects. Accurate and sensitive tetracycline detection methods are detrimental for monitoring residue levels in food and feedstock, waters, and in the environment. Such sensing strategies may be used to enforce regulatory tetracycline limits and support preventive or interventional actions against antibiotic resistance. Currently, detection technologies are focused on rapid quantitative measurements in various matrices[2,3]. Multiple sensing techniques are being developed, among which are chemosensors, fluorescent one being of particular interest for their high sensitivity and operational simplicity[4–8], electrochemical sensors, employing various types of detection probes like aptamers[9–11], metal-organic frameworks[12–14], nanoparticles[15–18], or colorimetric sensors

using different types of detection pathways[19–22]. Regardless of technology type, the general governing principle for all sensing platforms relays on employing tailored materials or molecular assemblies that enhance the trapping and selective recognition of tetracycline, contributing to improved sensing performance and detection limits. While recent advancements in state-of-the-art materials may offer improved sensitivity, practical applications are often dependent on the cost of production and availability of raw materials for scalable fabrication processes. Moreover, shelf-life stability is another key factor that greatly affects upscaling potential. We aimed at improving these three factors by developing a different type of detection probe. Tapping into a previously unexplored path, the rational development of N-substituted polyglycine oligomers, also known as peptoids, capable of forming complexes with tetracycline molecules could be a viable solution due to peptoids' easy synthesis, high availability of raw materials at low prices, and broad tailorability. On top of those aspects, as peptoids are peptidomimetic molecules, they benefit from similar structural properties to natural peptides, but without the drawback of biodegradability[23,24], due to the position of the substituent on the molecular backbone.

Peptoids were developed *via* submonomer solid-phase synthesis in 1992 by Zuckermann and colleagues[25], as peptidomimetic molecules, designed to overcome certain limitations of their natural counterparts, like susceptibility to proteolytic degradation and conformational rigidity. The method proposed allowed rapid, inexpensive and highly tailorable synthesis, benefiting from a very high yield[26]. The method involved two iterative steps per monomer unit, acetylation and nucleophilic substitution, performed on a solid resin support and utilizing primary amines as building blocks (Scheme 1). It allows the placement of the sidechain on the nitrogen atom, rather than the α-carbon[27]. This particularity results in the elimination of backbone hydrogen bonding, offering several advantages like increased stability, high chemical diversity and tunability of physiochemical properties and biological activity[27,28]. Moreover, since peptoids have higher conformational flexibility, we may expect a bigger diversity of complexation scenarios, making these molecules a very interesting fit for the development of capture probes. Solid phase synthesis can be fully automated using conventional peptide synthesizers, making industrial synthesis and use accessible[26,29].

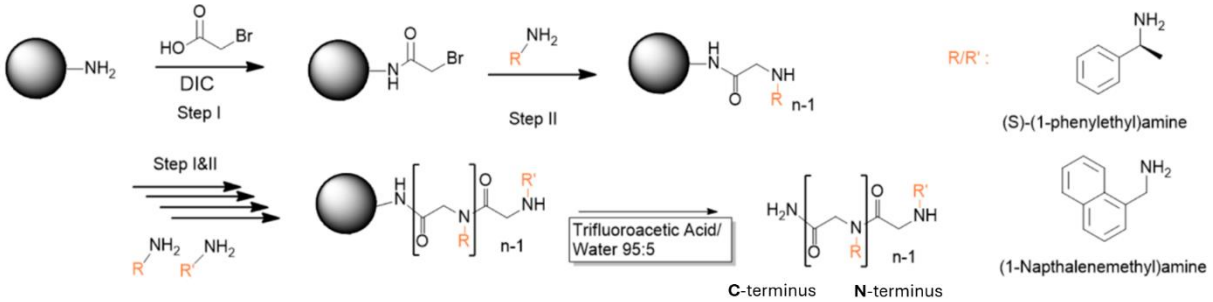

Scheme 1. General structure of peptoid oligomers and overview of their two-step solid-phase synthesis (acylation with activated bromoacetic acid, followed by nucleophilic displacement with a primary amine)

Given these advantages we chose to explore the possibility of rationally designing peptoid molecules that could be used as capture probes in the development of tetracycline sensors. Inspired from a previously described 8-mer aptamer which was reported to detect tetracycline in a colorimetric assay[20], we proposed that the use of helical peptoids would allow for a similar complexation. The proposed approach is aimed at mitigating the limitations associated with aptamer use (i.e. molecule stability and high costs), while maintaining small-molecule complexation possibility. Peptoids circumvent these limitations, having non-biodegradable backbone and easily scalable synthesis procedures using automated synthesis. The incorporation of bulky homochiral sidechains in the structure of peptoid oligomers has been an already-known strategy for helical conformation[30–33]. The presence of two consecutive N-(S)-(1-phenylethyl)glycine (Nspe) units at the N-terminus and another unit at the C-terminus plays an important role in helical folding[34,35]. Moreover, it has been previously reported that such peptoids assemble into polyproline-type helical structures[35,36], which is likely generated by n→π* interactions[37–39], or by coordination with other species in solution[40]. In recent years, work around helical-structured peptoids has focused on incorporating bulky non-aromatic side chains that induce preferential cis isomerization of the amide moiety, thus stabilizing the helical backbone arrangement.

In this work we have investigated a total of eight peptoid sequences which were developed in two parts. The initial set contained four peptoid sequences which have been synthesized containing two Nspe units at the C-terminus, followed by a unit with a bulky sidechain, other Nspe units and ending with another unit with a bulky sidechain, having counting between 50 and 71% Nspe units with increased periodicity, and adopting polyproline helical conformation. This conformation allows good interaction between distant side chains along the backbone, allowing the formation of a zone with increased tetracycline conjugation potential. Out of these four molecules, the one with the best conjugation capacity was selected for further investigations. For the second set we have synthesized four variants of this sequence, differing only in monomer units' order (Table 1), and have characterized their tetracycline complex formation in solution and in the gas phase.

Materials and Methods

Materials

Bromoacetic acid (BrAAc), acetonitrile (ACN), methanol (MeOH), (S)-(1-phenylethyl)amine (for the N-(S)-(1-phenylethyl)glycine – Nspe or S units), tetracycline

hydrochloride, diclofenac sodium salt, naproxen were purchased from Sigma Aldrich. 1-Methyl-2-pyrolidone (NMP, for peptide synthesis), acetaldehyde, magnesium sulphate (anhydrous) were obtained from VWR Chemicals, while ethyl acetate, dimethylformamide (DMF), dichloromethane (DCM), trifluoroacetic acid (TFA), sodium carbonate (anhydrous), were obtained from Fischer Scientific. We purchased N-methylpiperidine, 2-(aminomethyl)benzimidazole dihydrochloride hydrate (for the N-(benzimidazol-2-ylmethyl)glycine – Nbzi or I units), (1-Napthalenemethyl)amine (for the N-(1-Napthalenemethyl)glycine – N1npm or N units) from Thermo Scientific, tetrachloro-1,4-benzoquinone (chloranil), N,N'-Bis(isopropyl)carbodiimide (DIC) from Apollo Scientific and the Rink amide resin (100-200 mesh, substitution at filling: 0.51 mmole/g) from Novabiochem. Methylamine (for the N-(methyl)glycine – Nme or M units) was obtained from Acros Organics as 40% solution in water. All chemicals were used as received, unless otherwise specified. Ultrapure water (UPW) was obtained from a MiliQ ultrafiltration system.

Synthesis and purification

Peptoid synthesis

Peptoids were synthesized using a solid-phase synthesis procedure, adapted from somewhere else[41]. Rink amide resin (1 g) was swollen in 5 mL of NMP for 30 minutes at room temperature. Amine functional groups were FMOC-deprotected using 5 mL of N-methylpiperidine solution (20% in NMP). Iterative acetylation and nucleophilic substitution reactions were then used for the peptoid chain growth. Acetylation was carried out by adding 2.5 mL of DIC solution (2 M in NMP) and 2.5 mL of BrAAc solution (2 M in NMP) over the resin. Nucleophilic substitution was done by adding 5 mL of amine solution (1.5 M in NMP, unless specified otherwise) to the resin. After each synthesis step, the reaction mixture was evacuated, and the resin was washed five times with 5 mL of NMP. Reaction times for each step and type of agitation are specified below for the two procedures. After complete sequence synthesis, the resin was washed five times with NMP, followed by five times wash with DCM for drying. Resin was allowed to airdry overnight before peptoid cleavage. No unexpectedly high safety risks were encountered, however all synthesis reactions were carried out in a well-ventilated fume hood.

Table 1. Sequences of the synthesized peptoids initially and as PEP 1-NN variants (S: N-(S)-(1-phenylethyl)glycine, N: N-(1-Napthalenemethyl)glycine, I: N-(benzimidazol-2-ylmethyl)glycine, M: N-(methyl)glycine)

Initial peptoid sequences							
PEP 1-NN (i+4)	H_2N-S	S	N	S	S	S	N
PEP 2-IN	H_2N-S	S	I	S	S	S	N
PEP 3-II	H_2N-S	S	I	S	S	S	I
PEP 4-NMN	H_2N-S	$\mathbf{(S)_2}$	N	$\mathbf{(M)_3}$	N	S	S
PEP 1-NN sequence variations							

PEP 1-NN (i+1)	H_2N-S	S	N	N	S	S	S
PEP 1-NN (i+2)	H_2N-S	S	N	S	N	S	S
PEP 1-NN (i+3)	H_2N-S	S	N	S	S	N	S
PEP 1-N (i)	H_2N-S	S	N	S	S	S	S

a) High temperature

Initial peptoid synthesis was carried out as described previously[25] in a heated-mantle glass reactor, with a fritted bottom, at 80 °C. Agitation was achieved by nitrogen bubbling from below. After a 10-minute reaction to deprotect the Rink amide resin, the subsequent steps were carried out with reaction times of 10 minutes for acetylation and 15 minutes for nucleophilic substitution. These two steps were repeated according to the number of targeted monomer units. For the addition of the N-(S)-(1-phenylethyl)glycine, N-(1-Napthalenemethyl)glycine and N-(methyl)glycine) units, the amines used in the nucleophilic substitution were used as received, and the reaction was carried out in NMP under nitrogen bubbling. For the substitution involving 2-(aminomethyl)benzimidazole an initial neutralization of the hydrochloric acid was carried out using triethylamine, in a separate round bottom flask, and the substitution reaction was carried out in UPW, using mechanical agitation. A substitution reaction time of 30 minutes was used for this amine.

b) Room temperature

Purity test of the initial synthesis revealed that high temperature synthesis results in multiple side-products. Thus, the syntheses for the PEP 1-NN sequences variations were carried out at room temperature, with some modifications: chloranil testing was employed to check the presence (positive testing) or the absence of secondary amino end groups (negative testing) after certain synthesis steps. The reaction mixture was agitated magnetically. The FMOC-deprotection of the rink amide resin was repeated until a positive chloranil test was obtained. After each acetylation and nucleophilic addition, chloranil testing was employed, and the reaction times were prolonged until a negative or respectively a positive result were obtained. This led to a 30-minute reaction time for the FMOC-deprotection and acetylation steps and to a 120-minute reaction time for the nucleophilic addition steps. It is important to note that the highest possible reaction yield was desired, and while some shorter reaction times would have still yielded acceptable results, such a long reaction time was chosen to maximize the final synthesis yield. If needed, synthesis was interrupted after a nucleophilic addition step, the resin was rinsed with NMP, as per procedure, and thoroughly dried with DCM. To continue the reaction the following day, the resin was swollen again for 30 minutes in 5 mL of NMP, and the synthesis procedure was resumed.

Chloranil testing

The chloranil test procedure was performed on approximately 1 mg of dry resin, following a procedure adapted from somewhere else[42]. In short, 3 drops of both 0.8 mM chloranil solution in DMF and 2% acetaldehyde solution in DMF were allowed to interact with the

resin at room temperature for 5-10 minutes. A test was considered to give a positive result if the resin turned blue or purple, confirming the presence of terminal ammino groups on the surface of the resin beads.

Peptoid cleavage

After chain growth was completed, peptoids were cleaved from the resin using 95% TFA. For every approximately 100 mg of dry resin, 4 mL of TFA solution were used. The cleavage reaction was carried out for 30 minutes. The resin residue was eliminated and the resulting peptoid solution in TFA was neutralized using a 2 M sodium carbonate solution. The peptoids were then extracted in a separatory funnel using ethyl acetate. The organic layer was dried using anhydrous magnesium sulfate and evaporated. The crude peptoids were then subjected to further analysis or purification. Due to the highly corrosive nature of TFA, the cleavage procedure was carefully carried out in a well-ventilated fume hood, and the neutralization process was done considering the highly exothermic nature of the reaction. The sodium carbonate solution was added dropwise, to avoid any splashing risks.

Purification procedure

Crude peptoids were purified using a solid-phase extraction with gradient elution protocol, adapted from somewhere else[43]. Finisterre SPE C18 1000mg/12mL cartridges were used for the purification procedure. Prior to their use, the cartridges were activated using 15 mL of methanol and equilibrated using 15 mL of 60% ACN (0.1% TFA). Approximately 150 mg of crude peptoid were dissolved in 5 mL of the conditioning solvent and were loaded into the cartridge. The gradual peptoid elution was achieved by increasing the percentage of the ACN concentration with 5% percent from 60 to 40% and 30 to 0%, and a 1% increment from 39 to 30%. Each fraction, having a total volume of 15 mL, was collected and analyzed via RP-HPLC (Figure S6). The fractions containing the pure peptoid were combined and the organic solvent was evaporated. Due to the predominantly non-polar character of the molecule, as the ACN evaporated the peptoid molecules precipitated and were then separated by centrifugation followed by lyophilization.

Characterization

RP-HPLC was used to determine the purity of the peptoid samples before and after purification. Acetonitrile (0.1% TFA) and ultrapure water (0.1% TFA) were used as mobile phases, with a 100%-0% elution gradient for 30 min at 35 °C, using a 1 mL/min flow rate and a 10 µL injection volume. Chromatograms were recorded at five wavelengths 280, 254, 230, 220 and 214 nm (data only shown for 214 nm). An L-3000 HPLC system equipped with a DAD detector (Rigol Technologies Inc.) with a Kinetex EVO C18 column (150 × 4.6 mm, 5 µm particle size) from Phenomenex were used for the analysis.

Different mass spectrometric techniques were used in this study to assess either the successful synthesis of the peptoids, the formation of peptoid-analyte complexes and investigate their gas-phase survival yield, or the drift time of the peptoids and complexes in an ion mobility cell. Successful synthesis was investigated using a QExactive Orbitrap Mass spectrometer (Thermo Fischer) on the positive mode with a 140,000 resolution, 4.00 kV capillary voltage, 0.5 µA spray current, a 50.0 S-lens RF level and 320 ºC capillary temperature. For MS/MS experiments, fragmentation was performed in an HCD collision cell. Peptoid-analyte complex formation and survival yield as well as ion mobility experiments were carried out on a Synapt G2-S*i* (Waters, UK) mass spectrometer equipped with an ESI source and a traveling wave ion mobility cell using N_2 as drift gas at a pressure of 3 mbar. MS and MS/MS experiments were performed in positive mode, with a 3.1 kV capillary voltage, 80 ºC source temperature, 120 ºC desolvation gas temperature, 30 V sampling cone, 80 V source offset voltages and a 500 L/h desolvation gas flow. Ion Mobility Spectrometry (IMS) experiments were performed in positive mode in soft ionization conditions defined as capillary voltage of 2.5 kV, sampling cone voltage of 15 V, a source offset voltage of 50 V. The IMS travelling wave parameters are characterized by an IMS wave velocity of 550 m/s with a 33 V wave height. To determine the Collisional Cross Section (CCS), a custom calibration procedure was used, using PEG600, 1000, 2000, and 3350 g/mol commercially available from Sigma-Aldrich, as previously described[44].

All samples, 1 mg, were initially dissolved in 1 mL of 1:1 (ACN /UPW) and were diluted right before analysis to a 10 µM peptoid concentration. Methanol was added to a final concentration of 20% to improve the desolvation process. Complexes were analyzed as a 1:10 molar ratios peptoid:analyte.

Circular dichroism was used to assess the three-dimensional structure of the peptoid before and after their interaction with different analytes. A Jasco J-1500 spectrophotometer, equipped with an Xe lamp (150 W), was used for the measurements. Spectra were recorded in the 180-300 nm interval (1.00 nm bandwidth), with a 100 nm/min scanning speed (0.025 nm data pitch), 4 sec D.I.T. and 3 accumulations. Samples were analyzed in 1 mm path-length rectangular quartz cells, with a 0.1 mg/mL peptoid concentration in 1:1 (ACN /UPW). A background removal was performed, removing any solvent contribution for peptoid samples and any solvent-analyte contribution for peptoid-analyte samples. Complexes were analyzed as a 1:1 molar ratios peptoid:analyte.

Results and Discussion

The initial set of peptoid sequences were inspired from a short 8-mer ssDNA aptamer previously reported to have enhanced affinity towards tetracyclines[20]. The complexation, in this case, was reported to happen in a binding pocket formed between a cytosine and a guanine nucleotide, stabilized by analyte-base π-π stacking interactions and analyte-backbone H bonds. To mimic this type of stabilization, the peptoid sequences were

rationally designed to have a helical three-dimensional structure and glycine constituents that would promote π-π stacking interactions and H bonds with tetracycline. We have included Nspe units in key positions of the peptoid sequence to promote helical molecular arrangement and have used Nbzi and its guanine structural similarity and N1nmp units for its capability to promote and sustain π-π stacking interactions. Strategic positioning of the Nbzi an N1nmp along the peptoid chain, for the first set of four peptoid molecules, has been engineered to generate a gap between the sidechains that would accommodate tetracycline stacking, similarly to the stacking reported previously for the 8-mer ssDNA.

Figure 1-a depicts the initial peptoid sequences that were synthesized, according to the high-temperature SPS protocol. After successful synthesis confirmation (through MS/MS analysis, Figures S1-S4) their tetracycline complexation capacity was tested by full MS scan. PEP 1-NN was the only sequence for which *m/z* 1661 (corresponding to protonated complex containing tetracycline) was observed in the gas phase (Table S1). MS/MS analysis of *m/z* 1661 corresponding to $[PEP\ 1\text{-}NN+TET+H]^+$ showed fragments of the peptoid and tetracycline, confirming that the observed signal was indeed a complex between the two components. Thus, the PEP 1-NN peptoid was selected for further sequence investigation. However, HPLC analysis of the peptoid revealed the presence of multiple reaction products (Figure S5), which was attributed to the SPS conditions used. To minimize side reactions, subsequent syntheses were carried out under milder reaction conditions, following the room-temperature SPS protocol.

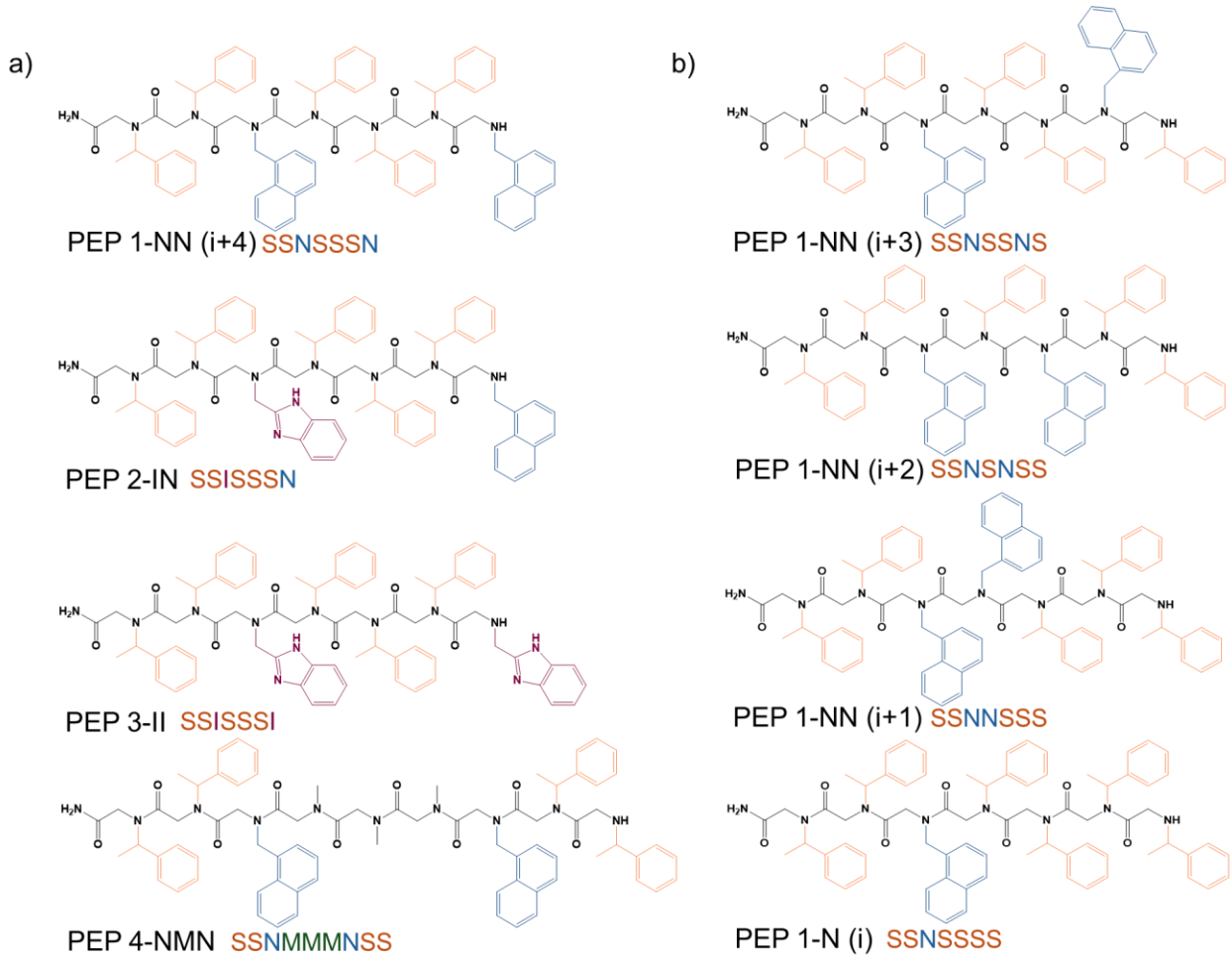

Figure 1. Sequences of the peptoid molecules synthesized: (a) Initial candidates obtained using the high-temperature SPS protocol, and (b) new candidates synthesized using the room-temperature SPS protocol after selecting the most promising side chain for tetracycline interaction.

Based on the MS spectra of the different candidates shown in Figure 1-a, only peptoids bearing naphthyl pendant groups exhibited non-covalent interactions with the target molecule (tetracycline), namely PEP 1-NN, highlighting the importance of π-π stacking interactions, similar to the 8-mer ssDNA, but regardless of sidechain structural similarity to the nucleotide bases. Consequently, only peptoids with this specific side chain were further investigated. To assess the influence of the pendant group's position along the backbone, four additional sequences were synthesized using the room-temperature SPS protocol. Their sequences are depicted in Figure 1-b. The position of the N1npm unit closer to the C-terminus was kept constant throughout the additional sequences, while the position second of the N1npm unit was changed, creating the PEP 1-NN (i+x) variations, making the initial PEP 1-NN be the (i+4) variant. This decision was made in order to investigate whether the relative position of the two naphthyl sidechains would play a role in complexation capacity, while maintaining the structural considerations for

polyproline helical conformation of the peptoid backbone. A PEP 1-N (i) variant was synthesized to test whether a second N1npm unit was necessary for complexation to occur. Structural confirmation for all the five variants was obtained using MS/MS (Figures S13-S17).

Prior to complexation experiments, the five PEP 1-NN variants were purified utilizing a modified SPE procedure, as described in the Methods section. Pure peptoids (Figure S7) were then subjected to complexation experiments using Mass Spectrometry techniques and Circular Dichroism.

Mass Spectrometry

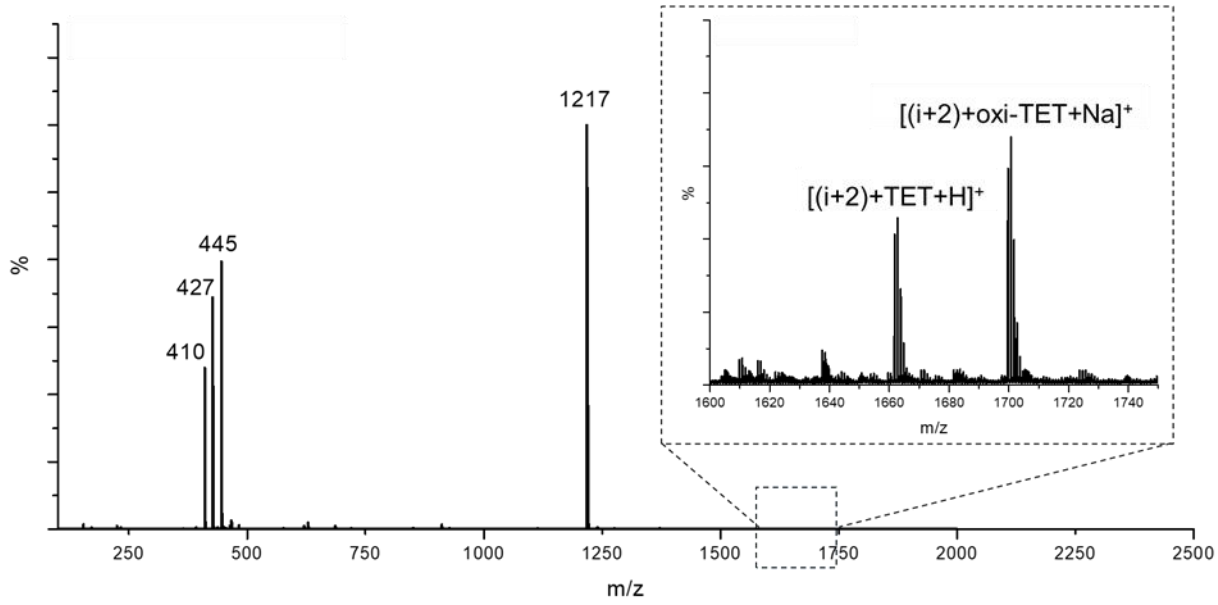

Figure 2. Recorded mass spectrum of the PEP 1-NN (i+2) (SSNSNSS) variant in the presence of tetracycline (TET), insert, magnification between *m/z* 1600 and *m/z* 1750, showing the complexes formed between the two components, either as [Peptoid+Tetracycline+H]$^+$ (*m/z* 1661) or [Peptoid+oxi-Tetracycline+Na]$^+$ (*m/z* 1699).

Following the purification and characterization of the peptoids, various mass spectrometry analyses of the complexes formed were performed. Initial full MS spectra of all peptoid variants in the presence of tetracycline (Figure 2 and Figures S8-S12) showed two *m/z* corresponding to complexes: [Peptoid+Tetracycline+H]$^+$ (*m/z* 1661) and [Peptoid+oxi-Tetracycline+Na]$^+$ (*m/z* 1699). Since the technical requirements for the MS analysis ask for a very low sample concentration, we have first prepared the sample as 1 mg/mL concentration, followed by appropriate dilution, which could otherwise affect the intensity of the complex ions. Nevertheless, these ions could still be detected and their MS/MS analysis showed fragments corresponding to both tetracycline, peptoid, and their specific

fragments (analyte and peptoid), confirming the identity of the complexes (Figure 3 and Figures S13-S17).

An interesting phenomenon was observed due to this analysis: *m/z* of a complex with peptoid, teracycline and one oxygen atom was detected as a sodium cationized species. While it may initially look like a single-atom oxidation of tetracycline[45], this oxidation phenomenon was reported only as a result of UV irradiation. Indeed, as reported in Figure 3, MS/MS spectra confirms either specific fragment of peptoid alone after side chain loss (SCL)[46] *m/z* 1077 and complex after analyte elimination with one oxygen more (*m/z* 1255).

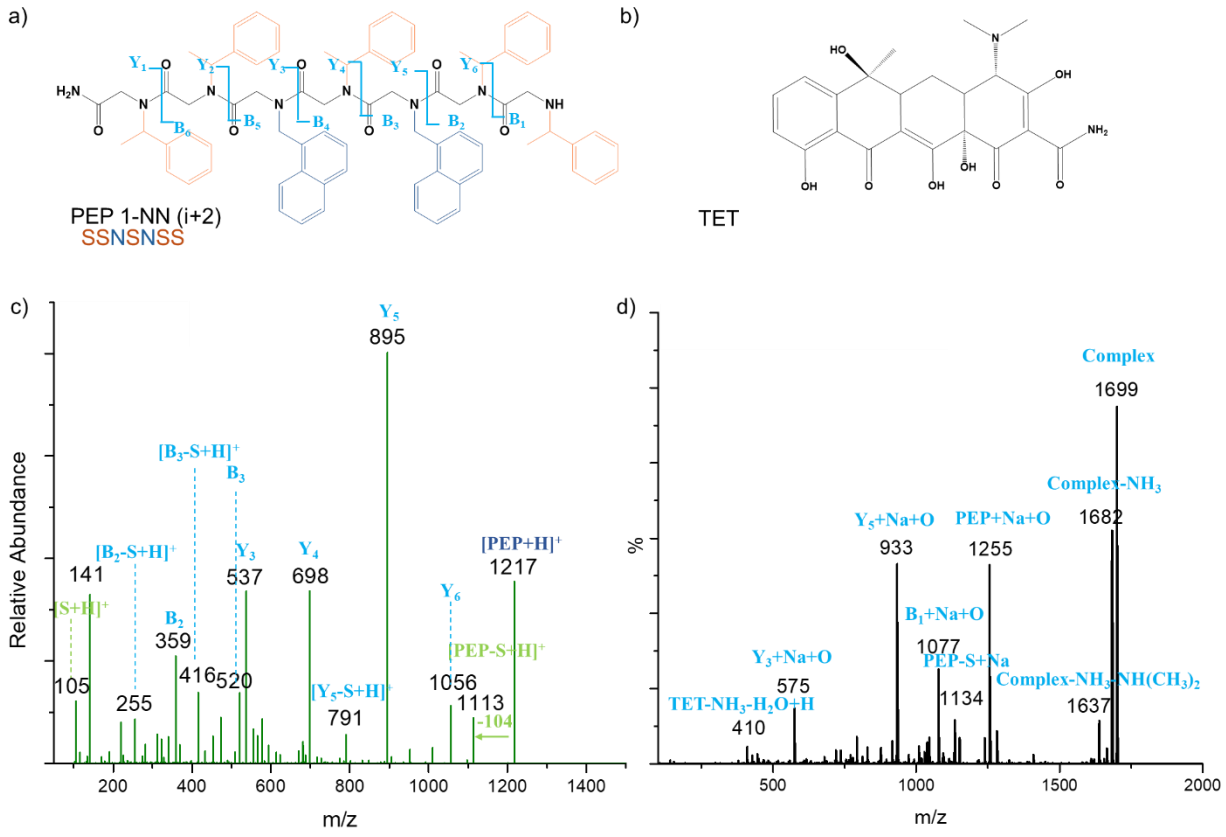

Figure 3 a) PEP 1-NN (i+2) variant structure, highlighting B-Y fragmentation patterns, b) tetracycline structure, c) MS/MS *m/z* 1217 (PEP 1-NN (i+2).H^+), highlighting the most notable *m/z* values attribution and d) MS/MS of the sodiated complex between the PEP 1-NN (i+2) variant and oxidized tetracycline

Fragmentation patterns of all sodium-cationized complexes show an initial loss of tetracycline moieties (NH_3 and $NH(CH_3)_2$) followed by a second fragmentation leading to a complete removal of tetracycline. Interestingly, the complete removal of tetracycline does not result in an oxygen atom loss, rather the oxygen atom “stays” with the peptoid ions, suggesting the possibility to transfer the oxygen from the oxidized Tetracycline (oxi-

Tetracycline) to the peptoid. Table S2 summarizes the most intense signals observed in the MS/MS analysis and their corresponding attribution. Interestingly, for PEP 1-NN (i+3) the fragmentation pattern shows a signal with a *m/z* value of 1408, which may be attributed to a fragment of the complex containing a fragment of the tetracycline molecule with a mass of 153u. While this fragmentation pattern of tetracycline has been reported before[47], the fact that this fragment can be detected only in the case of the (i+3) complex could suggest a better stability of the complex with this peptoid variant.

We have also looked at the protonated peptoid-tetracycline complexes. While these species did not have the same intensity in the full MS spectra, the fact that they could still be detected for most of the variants caught our attention. In this case, the PEP 1-N (i) variant did not show any complex, suggesting that two naphthalene sidechains would be necessary for this complexation to occur (Figures S8-S12). MS/MS analysis of these complexes was also performed (data not shown), revealing that they are significantly more fragile and undergo extensive fragmentation at very low collision voltages (<15 V). This sensitivity is typically observed for protonated species compared to their sodium-cationized counterparts. For additional analyses, such as survival yield investigations and ion mobility spectrometry characterization, we focused on more stable complexes to avoid undesired fragmentation that could lead to a loss of sensitivity. Additionally, it is interesting to point out that only complexes with oxidized tetracycline are observed, it could suggest the oxidation helps to create the sodiated ions.

Survival yield

Further, we have performed survival yield experiments for the sodiated complexes to evaluate their gas phase stability. Experiments were performed in the 0 – 60 V collisional voltage (CV) range and the results are depicted in Figure 4. All complexes showed similar results, the only difference arising for the complex ions with PEP 1-NN (i+1) variant, whose starting point was lower than for the rest of the variants, fragments being already visible at CV=0 V.

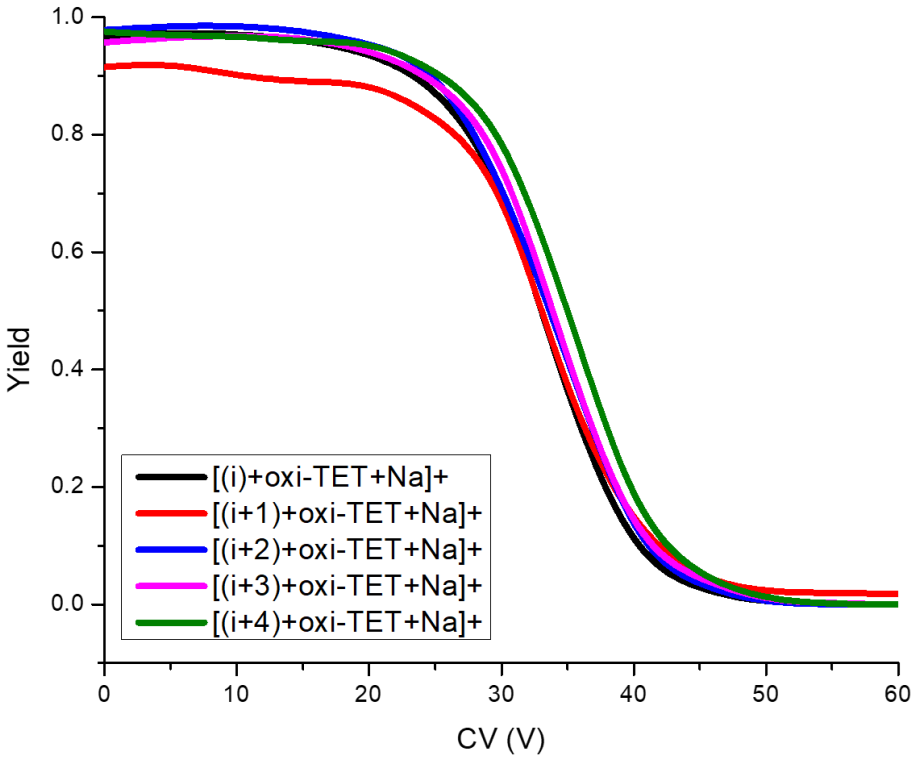

Complex	$CV_{1/2}$(V)
(i)	33.4
(i+1)	34.0
(i+2)	33.8
(i+3)	34.3
(i+4)	35.1

Figure 4. Survival yield of the sodiated complexes formed between the peptoid variants and oxidized tetracycline (normalized to the total ion count)

The collision voltage required to fragment 50% of precursor ions ($CV_{1/2}$) was determined, leading to the main conclusion that all complexes exhibit similar kinetic stability, although the PEP 1-NN (i+4) TET isomer ions show a higher $CV_{1/2}$ value. In addition to survival yield curves, appearance curves, representing the intensity of fragments generated during complex dissociation, are reported in Figure 5 and Figure S18. The initial loss of ammonia has very similar CV value for all variants, while the additional loss of the $NH(CH_3)_2$ tetracycline moiety is accentuated for the complexes of PEP 1-NN (i+3) and (i+4) (Figure 5). Moreover, complete removal of the non oxidized analyte from the complex happens in a similar manner for all variants, with the exception of PEP 1-NN (i+4), for which the intensity is almost 50% decreased than for the rest. Both observations suggest a better retention of tetracycline for this sequence. When it comes to peptoid backbone fragments, we see that all isomers require high CV values and that PEP 1-NN (i+2) shows the highest intensity for Y_5 and Y_3 fragments. PEP 1-NN (i+4) and (i+3) complex samples show modest intensity for backbone fragmentation. Since the interaction between the analyte and the peptoids is particularly strong and backbone fragmentation appears to occur only after complete analyte removal, fragmentation of the peptoid backbone is less observed for the PEP 1-NN (i+3) and (i+4) isomers in the current CV range.

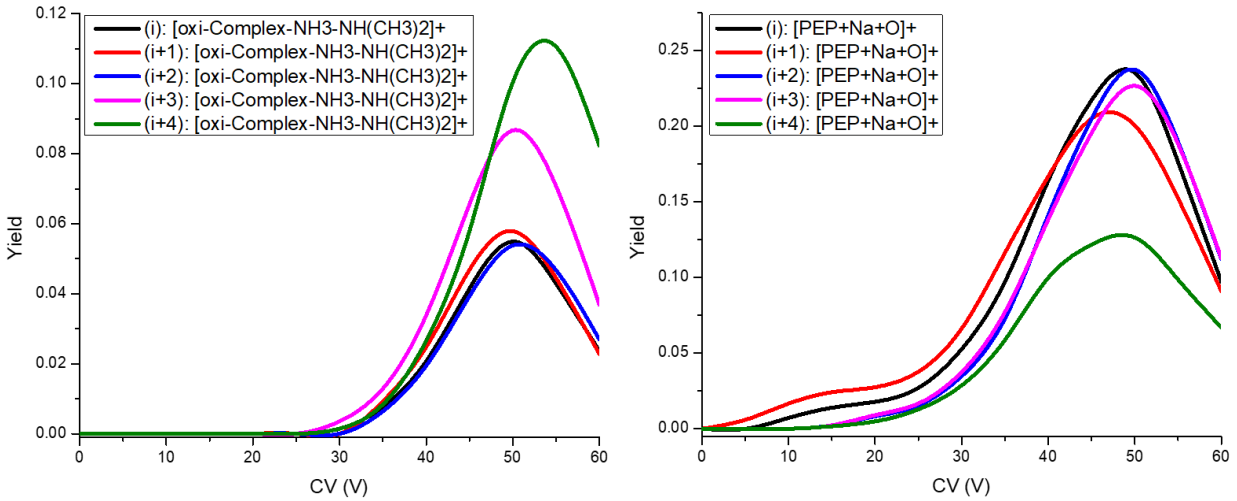

Figure 5. Survival yield of the sodiated complexes' fragments formed between the peptoid variants and oxidized tetracycline (normalized to the total ion count and corrected with the survival yield of the complex at CV 0V); left graph corresponds to the appearance of *m/z* 1601 for PEP 1-N (i) and 1637 for the PEP 1-NN (i+x) variants, while the right graph corresponds to the appearance of *m/z* 1219 for PEP 1-N (i) and 1255 for the PEP 1-NN (i+x) variants.

While this investigation is useful for assessing the overall gas phase stability of the complexes, the fragments' intensities provide some insight into "fragile points" of the complexes. We observe a stronger bond and a preference of oxi-TET for PEP1-NN (i+4), both through the $CV_{1/2}$ value and also through the reduced intensity for the $[PEP+O+Na]^+$ fragments, compared to the rest of the variants. Meanwhile, fragmentation patterns of oxi-complex ions of the PEP 1-NN (i+2) variant show a higher peptoid backbone fragmentation, with a smaller $CV_{1/2}$ value. Oxi-complexes of PEP 1-NN (i+3) variant on the other hand have an intermediate $CV_{1/2}$ value, while exhibiting reduced backbone fragmentation and intermediate $-NH(CH_3)_2$ tetracycline moiety loss. These results highlight firstly that peptoid sequence affects complex strength, and secondly that while the interaction is noncovalent, the fact that we can detect fragments in the gas phase from the two components demonstrates the strength of the association in gas phase.

Ion mobility spectrometry

The ion mobility results provide some insights into the complex architecture in the gas phase (Figure 6). Firstly, we notice a slight shift in the CCS value from PEP 1-N (i) to the PEP 1-NN (i+x) variants which is due to the difference in the number of N1npm sidechains, which can be further seen for their complexes. There does not seem to be significant difference between the different PEP 1-NN (i+x) variants due to their isomeric

structure. For the sodiated complexes, knowing that tetracycline CCS value is 139 Å² (data not shown), the fact the CCS value of the complexes is significantly smaller than the sum of the variants' and tetracycline's CCS values is an indication of an interaction with a possible structural modification. There was no remarkable difference between sodiated complexes of the different variants, which could be attributed to a gas-phase compaction sometimes resulting in identical CCS values despite structural differences, this trend being previously reported[48]. In order to confirm the structural modification and have better insight into the complexation behavior in solution, we have further performed Circular Dichroism (CD) measurements.

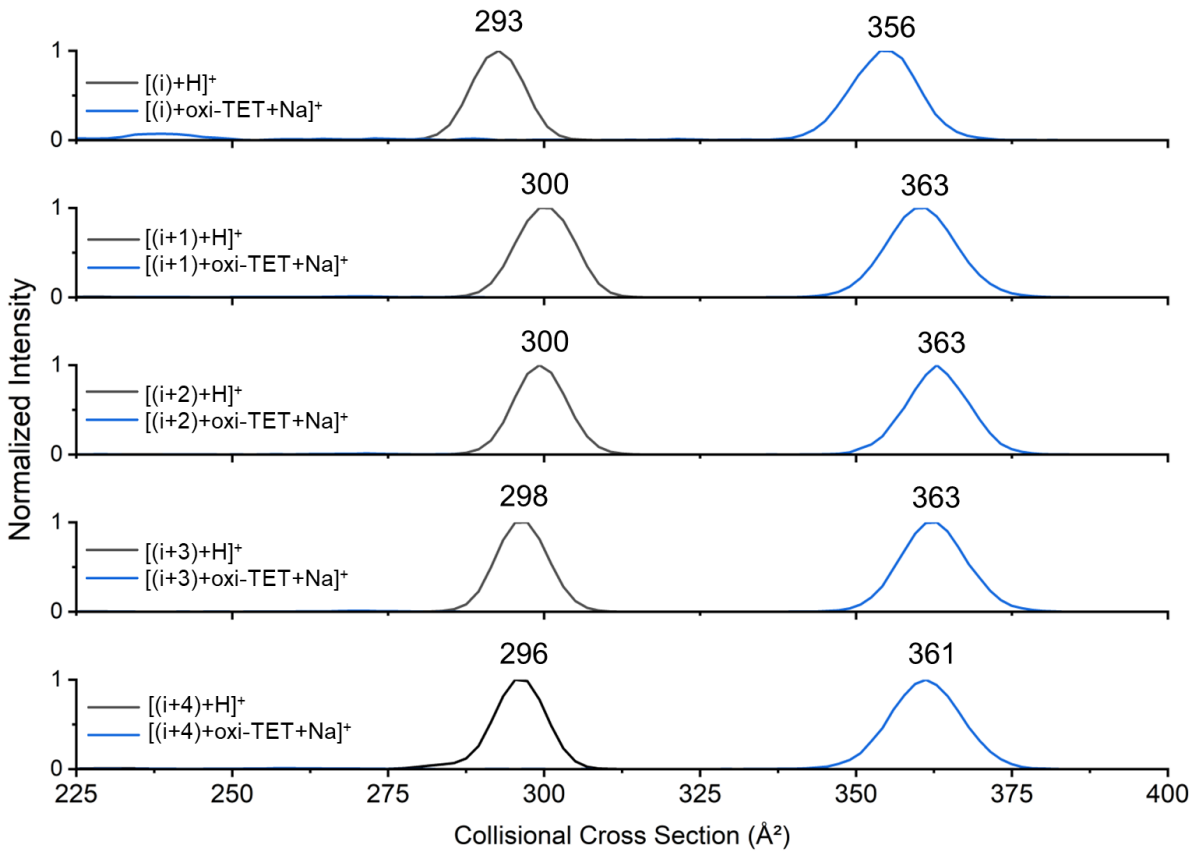

Figure 6. IMS results for the protonated peptoids (black) and their sodium cationized complexes with oxidized tetracycline (blue)

Circular Dichroism

CD analysis revealed some differences in the solution three-dimensional configuration of the five PEP 1-NN structural variations. While all of them showed helical backbone conformation, some differences were observed, as reported in Figure 7a. While the PEP 1-N (i) and PEP 1-NN (i+4) variants have very typical helical structural motifs, the other

three sequences show differences in the 200-230 nm region. These structural particularities were expected, with regards to the selection of the units. As the N1npm units contain naphthalene groups, exciton couples were expected. Interestingly, considering that the pendant naphthalene groups are connected to the backbone through a highly flexible CH_2 unit, stronger exciton couplets are observed for the PEP 1-NN (i+1) and (i+2) variants, which exhibit the greatest proximity of the N1nmp units, the latter of those showing a distinct CD spectra, where the contribution of the couplet has the most drastic effect on the overall result. Even though the Nspe units promote the formation of helical conformations with a pitch of 3^{49} , thus more favorable π-π stacking interactions for the PEP 1-NN (i+3) variant, the vertical distance between the two naphthalene groups played a role in diminishing couplet strength.

Peptoids' interaction with tetracycline was then studied in solution using CD. Diclofenac and naproxen were used as control analytes, as shown in Figure 7-b. While the secondary structure of the peptoids did not seem to vary after interaction with tetracycline, a variation of the CD signal in the 250-300 nm region was observed for all peptoid variants. A positive exciton couplet centered around 277 nm is observed in the near-UV region, with rotational strength increasing in the PEP 1-NN (i+4), (i+3), (i+1), (i+2) order. As this exciton coupling is observed only in the near-UV region, it could indicate the formation of a conjugate between the peptoid sequences and tetracycline with a distinct tertiary structure, having a positive chirality. The formation of this conjugate seems to be induced by the presence of two naphthalene side groups, suggesting a possible π-π stacking interaction involving two N1nmp groups and tetracycline. None of the peptoid sequences were observed to conjugate either diclofenac or naproxen, despite their structural similarities, suggesting a preference for tetracycline conjugation. These preliminary control tests highlight the possible peptoids' affinity for the linearly fused A-D tetracyclic ring architecture, compared to smaller non-fused analogues, despite containing aromatic moieties.

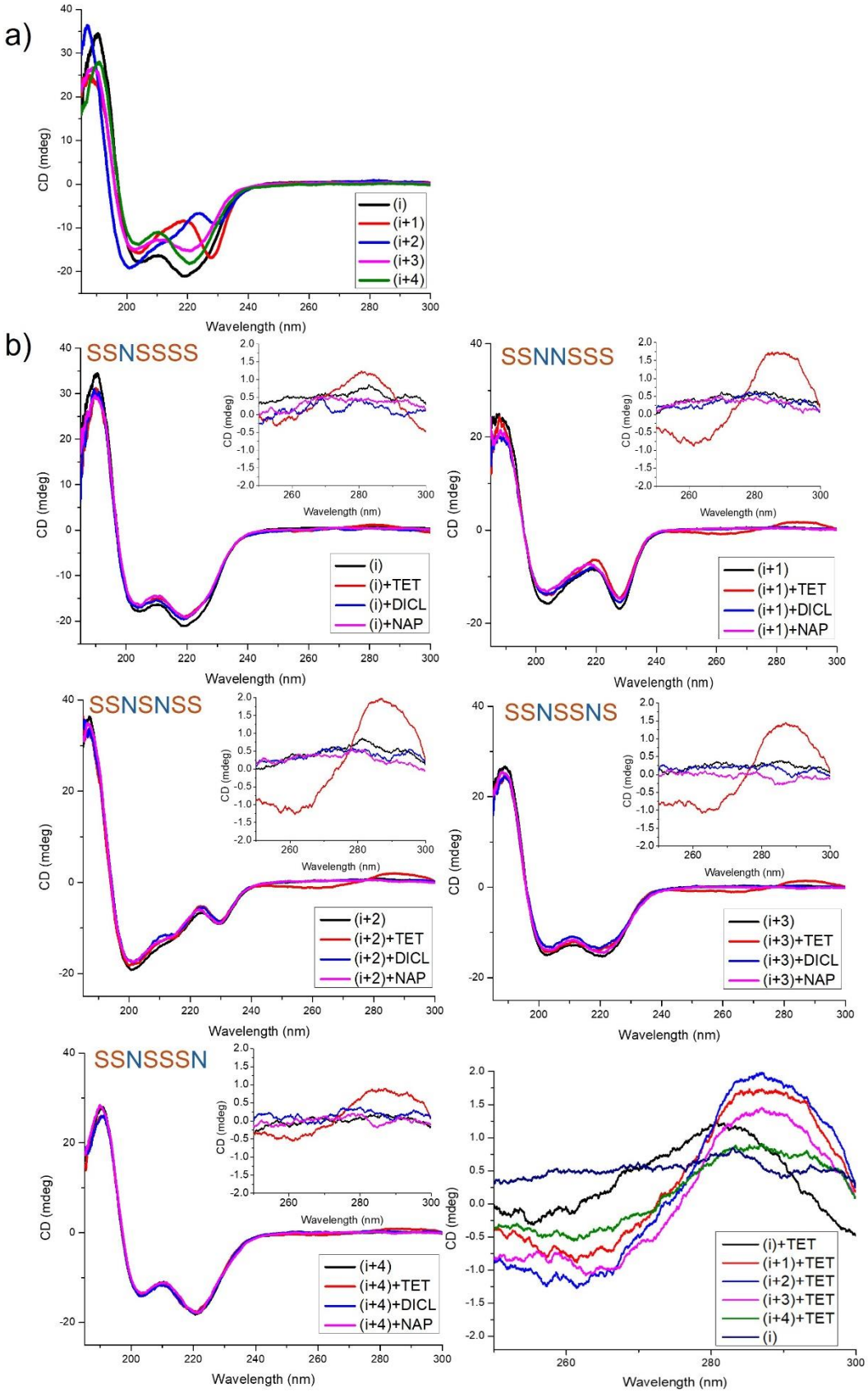
a)
CD (mdeg)
Wavelength (nm)
(i)
(i+1)
(i+2)
(i+3)
(i+4)
b)
SSNSSSS
(i)
(i)+TET
(i)+DICL
(i)+NAP
SSNNSSS
(i+1)
(i+1)+TET
(i+1)+DICL
(i+1)+NAP
SSNSNSS
(i+2)
(i+2)+TET
(i+2)+DICL
(i+2)+NAP
SSNSSNS
(i+3)
(i+3)+TET
(i+3)+DICL
(i+3)+NAP
SSNSSSN
(i+4)
(i+4)+TET
(i+4)+DICL
(i+4)+NAP
(i)+TET
(i+1)+TET
(i+2)+TET
(i+3)+TET
(i+4)+TET
(i)

Figure 7 a) Circular dichroism spectra of the five PEP 1-NN variants, using 1:1 (ACN /UPW) as solvent b) Circular dichroism spectra of the five PEP 1-NN variants in the absence and presence of tetracycline, diclofenac and naproxen (insert and last panel showing the 250-300 nm region), using 1:1 (ACN /UPW) as solvent

Conclusion and perspectives

In this study we aimed to design peptoid molecules that are able to form complexes with tetracycline. The peptoid structures were inspired by a very short aptamer which was previously reported to selectively conjugate the desired analyte, and we have thus chosen to design helical sequences containing monomer units that would best promote complexation via π-π stacking interactions and hydrogen bonding. We initially synthesized four peptoids with different sidechains from which we have selected the one that showed some preliminary complexation properties. We have then investigated how its sequence affects the complexation both in gas phase and in solution.

Mass spectrometry has highlighted that indeed the complexation is achieved, and interestingly, sodium cationized adducts between the peptoid molecules and oxidized tetracycline are detected. MS/MS investigation as well as IMS showed that what we detect in the gas phase is a true stable complex that is formed. Additionally, IMS experiments confirmed the presence of complexes with significant lower CCS to prove structural rearrangement and could suggest a sandwich insertion of tetracycline between the naphthyl side chains. This fact was also highlighted by CD, which provided insight into the solution behavior, showing that the peptoid sequence has a significant effect on the rotational strength of the exciton. To gain a better understanding of the nature of the interaction between these peptoid sequences and tetracycline further experiments on a more resolved Ion Mobility spectrometer and will be performed on the new Cyclic series recently installed in Mons. Additionally, molecular dynamics simulations can provide more insights into the three-dimensional arrangement of the complexes and compare to ion mobility results.

Acknowledgements

The authors would like to thank Prof. Celine Henoumont and Dr. Matei D. Raicopol for the insightful discussions that greatly contributed to this study. This collaborative work was supported by a grant of the Ministry of Research, Innovation and Digitalization, CCCDI - UEFISCDI, project number PN-IV-P8-8.3-PM-RO-BE-2024-0010, within PNCDI IV, contract number 6BMBE/2025, BioMimAntiCx. The Mass spectrometry results obtained using the QExactive Orbitrap Mass spectrometer, as well as the Circular Dichroism measurements were possible due to the project INOVABIOMED, European Regional Development Fund through Competitiveness Operational Program 2014–2020 (ID P_36_611). The S2MOs is grateful to the Fonds National de la Recherche Scientifique

for continuing support and for the acquisition of Synapt G2-Si. L.G. thanks the UMONS for the PhD grant in the frame of the ARC project.

Supporting Information: MS/MS spectra for all synthesized peptoid molecules and for the complexes between tetracycline and the PEP 1-NN variants, RP-HPLC chromatograms showing the crude and purified peptoid samples, MS results for the PEP 1-NN variants in the presence of tetracycline and survival yield of investigated complexes

References

(1) Nelson, M. L.; Levy, S. B. The History of the Tetracyclines. *Ann. N. Y. Acad. Sci.* **2011**, *1241* (1), 17–32. https://doi.org/https://doi.org/10.1111/j.1749-6632.2011.06354.x.

(2) Onaş, A. M.; Dascălu, C.; Raicopol, M. D.; Pilan, L. Critical Design Factors for Electrochemical Aptasensors Based on Target-Induced Conformational Changes: The Case of Small-Molecule Targets. *Biosensors (Basel).* **2022**, *12* (10). https://doi.org/10.3390/bios12100816.

(3) Madej, M.; Knihnicki, P.; Porada, R.; Kochana, J. (Bio)Electroanalysis of Tetracyclines: Recent Developments. *Biosensors (Basel).* **2025**, *15* (2). https://doi.org/10.3390/bios15020101.

(4) Guo, J.; Xin, J.; Wang, J.; Li, Z.; Yang, J.; Yu, X.; Yan, M.; Mo, J. A High-Efficiency and Selective Fluorescent Assay for the Detection of Tetracyclines. *Sci. Rep.* **2024**, *14* (1), 22918. https://doi.org/10.1038/s41598-024-74411-7.

(5) Yang, L.; Wang, X.; Zhang, F.; Yu, L.; Bai, B.; Zhang, J.; Zhang, B.; Tian, Y.; Qin, S.; Yang, Y. Two Birds with One Stone: A Universal Design and Application of Signal-on Labeled Fluorescent/Electrochemical Dual-Signal Mode Biosensor for the Detection of Tetracycline Residues in Tap Water, Milk and Chicken. *Food Chem.* **2024**, *430*, 136904. https://doi.org/https://doi.org/10.1016/j.foodchem.2023.136904.

(6) Wang, J.; Qin, Y.; Ma, Y.; Meng, M.; Xu, Y. Low-Toxicity and High-Stability Fluorescence Sensor for the Selective, Rapid, and Visual Detection Tetracycline in Food Samples. *Molecules* **2024**, *29* (24). https://doi.org/10.3390/molecules29245888.

(7) John, B. K.; John, N.; Korah, B. K.; Thara, C.; Abraham, T.; Mathew, B. Nitrogen-Doped Carbon Quantum Dots as a Highly Selective Fluorescent and Electrochemical Sensor for Tetracycline. *J. Photochem. Photobiol. A Chem.* **2022**, *432*, 114060. https://doi.org/https://doi.org/10.1016/j.jphotochem.2022.114060.

(8) Basak, M.; Das, G. Fluorescent Sensors for Tetracycline Detection in Aqueous Medium: A Mini-Review. *Chem. Asian J.* **2024**, *19* (15), e202400406. https://doi.org/https://doi.org/10.1002/asia.202400406.

(9) Song, J.; Lin, X.; Jiang, N.; Huang, M. Carbon-Doped WO3 Electrochemical Aptasensor Based on Box-Behnken Strategy for Highly-Sensitive Detection of Tetracycline. *Food Chem.* **2022**, *367*, 130564. https://doi.org/https://doi.org/10.1016/j.foodchem.2021.130564.

(10) Huo, J.; Guo, R.; Yin, J.; Liu, Y.; Zhang, Y.; Ruan, F.; Shi, Y.; Li, Y. Nanomaterial-Modified Electrochemical Aptasensors for Tetracycline Detection: A Review. *Analyst* **2025**, *150* (12), 2453–2468. https://doi.org/10.1039/D5AN00097A.

(11) Benvidi, A.; Nikmanesh, M.; Dehghan Tezerjani, M. Graphene Oxide/Chitosan Based Impedimetric Aptasensor Along with an Ester Linker for the Detection of Tetracycline. *Journal of Nanostructures* **2022**, *12* (1), 213–223. https://doi.org/10.22052/JNS.2022.01.020.

(12) Liang, N.; Hu, X.; Zhang, X.; Li, W.; Guo, Z.; Huang, X.; Li, Z.; Zhang, R.; Shen, T.; Zou, X.; Shi, J. Ratiometric Sensing for Ultratrace Tetracycline Using Electrochemically Active Metal–Organic Frameworks as Response Signals. *J. Agric. Food Chem.* **2023**, *71* (19), 7584–7592. https://doi.org/10.1021/acs.jafc.3c00846.

(13) Sankhla, L.; Kumar, A.; Kushwah, H. S. Electrochemical Detection of Tetracycline Using Cu-MOF Functionalised Screen-Printed Electrodes. *Sci. Rep.* **2025**, *15* (1), 19129. https://doi.org/10.1038/s41598-025-03150-0.

(14) Han, Q.; Shi, X.; Kang, K.; Cao, Y.; Cong, L.; Wang, J. Silver Nanoparticles In Situ Enhanced Electrochemiluminescence of the Porphyrin Organic Matrix for Highly Sensitive and Rapid Monitoring of Tetracycline Residues. *J. Agric. Food Chem.* **2024**, *72* (16), 9498–9506. https://doi.org/10.1021/acs.jafc.4c01525.

(15) Kushikawa, R. T.; Silva, M. R.; Angelo, A. C. D.; Teixeira, M. F. S. Construction of an Electrochemical Sensing Platform Based on Platinum Nanoparticles Supported on Carbon for Tetracycline Determination. *Sens. Actuators B Chem.* **2016**, *228*, 207–213. https://doi.org/https://doi.org/10.1016/j.snb.2016.01.009.

(16) Zeb, S.; Wong, A.; Khan, S.; Hussain, S.; Sotomayor, M. D. P. T. Using Magnetic Nanoparticles/MIP-Based Electrochemical Sensor for Quantification of Tetracycline in Milk Samples. *Journal of Electroanalytical Chemistry* **2021**, *900*, 115713. https://doi.org/https://doi.org/10.1016/j.jelechem.2021.115713.

(17) Lai, M.; Huang, L.; Wang, C.; Zuo, R.; Liu, J. Preparation of Electrochemical Sensors Based on Graphene/Ionic Liquids and the Quantitative Detection and Toxicity Evaluation of Tetracycline. *Nanomaterials* **2025**, *15* (4). https://doi.org/10.3390/nano15040263.

(18) Elamin, M. B. Design of Novel Electrochemical Sensor Functionalized with Green Nanoparticles for Tetracycline Monitoring. *Polym. Adv. Technol.* **2024**, *35* (8), e6543. https://doi.org/https://doi.org/10.1002/pat.6543.

(19) Gong, X.; Li, X.; Qing, T.; Zhang, P.; Feng, B. Amplified Colorimetric Detection of Tetracycline Based on an Enzyme-Linked Aptamer Assay with Multivalent HRP-Mimicking DNAzyme. *Analyst* **2019**, *144* (6), 1948–1954. https://doi.org/10.1039/C8AN02284D.

(20) Kwon, Y. S.; Ahmad Raston, N. H.; Gu, M. B. An Ultra-Sensitive Colorimetric Detection of Tetracyclines Using the Shortest Aptamer with Highly Enhanced Affinity. *Chem. Commun.* **2014**, *50* (1), 40–42. https://doi.org/10.1039/C3CC47108J.

(21) Cui, Y.; Zhao, N.; Wang, S.; Yan, H.; Han, D. Colorimetric Detection of Tetracycline by Enhancing Peroxidase-like Activity of Polymerized MnO2@ZIF-67 Nanocomposites. *Biosens. Bioelectron.* **2025**, *287*, 117726. https://doi.org/https://doi.org/10.1016/j.bios.2025.117726.

(22) Chatten, L. G.; Krause, S. I. Colorimetric Assay of Tetracycline Antibiotics. *J. Pharm. Sci.* **1971**, *60* (1), 107–110. https://doi.org/10.1002/jps.2600600121.

(23) Schunk, H. C.; Austin, M. J.; Taha, B. Z.; McClellan, M. S.; Suggs, L. J.; Rosales, A. M. Oxidative Degradation of Sequence-Defined Peptoid Oligomers. *Mol. Syst. Des. Eng.* **2023**, *8* (1), 92–104. https://doi.org/10.1039/D2ME00179A.

(24) Mojsoska, B.; Carretero, G.; Larsen, S.; Mateiu, R. V.; Jenssen, H. Peptoids Successfully Inhibit the Growth of Gram Negative E. Coli Causing Substantial Membrane Damage. *Sci. Rep.* **2017**, *7* (1), 42332. https://doi.org/10.1038/srep42332.

(25) Zuckermann, R. N.; Kerr, J. M.; Kent, S. B. H.; Moos, W. H. Efficient Method for the Preparation of Peptoids [Oligo(N-Substituted Glycines)] by Submonomer Solid-Phase Synthesis. *J. Am. Chem. Soc.* **1992**, *114* (26), 10646–10647. https://doi.org/10.1021/ja00052a076.

(26) Clapperton, A. M.; Babi, J.; Tran, H. A Field Guide to Optimizing Peptoid Synthesis. *ACS Polymers Au* **2022**, *2* (6), 417–429. https://doi.org/10.1021/acspolymersau.2c00036.

(27) Sun, J.; Zuckermann, R. N. Peptoid Polymers: A Highly Designable Bioinspired Material. *ACS Nano* **2013**, *7* (6), 4715–4732. https://doi.org/10.1021/nn4015714.

(28) Chan, B. A.; Xuan, S.; Li, A.; Simpson, J. M.; Sternhagen, G. L.; Yu, T.; Darvish, O. A.; Jiang, N.; Zhang, D. Polypeptoid Polymers: Synthesis, Characterization, and Properties. *Biopolymers* **2018**, *109* (1), e23070. https://doi.org/https://doi.org/10.1002/bip.23070.

(29) Zuckermann, R. N. Peptoid Origins. *Peptide Science* **2011**, *96* (5), 545–555. https://doi.org/https://doi.org/10.1002/bip.21573.

(30) Kirshenbaum, K.; Barron, A. E.; Goldsmith, R. A.; Armand, P.; Bradley, E. K.; Truong, K. T. V; Dill, K. A.; Cohen, F. E.; Zuckermann, R. N. Sequence-Specific Polypeptoids: A Diverse Family of Heteropolymers with Stable Secondary Structure. *Proceedings of the National Academy of Sciences* **1998**, *95* (8), 4303–4308. https://doi.org/10.1073/pnas.95.8.4303.

(31) Armand, P.; Kirshenbaum, K.; Goldsmith, R. A.; Farr-Jones, S.; Barron, A. E.; Truong, K. T. V; Dill, K. A.; Mierke, D. F.; Cohen, F. E.; Zuckermann, R. N.; Bradley, E. K. NMR Determination of the Major Solution Conformation of a Peptoid Pentamer with Chiral Side Chains. *Proceedings of the National Academy of Sciences* **1998**, *95* (8), 4309–4314. https://doi.org/10.1073/pnas.95.8.4309.

(32) Wu, C. W.; Sanborn, T. J.; Zuckermann, R. N.; Barron, A. E. Peptoid Oligomers with α-Chiral, Aromatic Side Chains: Effects of Chain Length on Secondary Structure. *J. Am. Chem. Soc.* **2001**, *123* (13), 2958–2963. https://doi.org/10.1021/ja003153v.

(33) Armand, P.; Kirshenbaum, K.; Falicov, A.; Dunbrack, R. L.; Dill, K. A.; Zuckermann, R. N.; Cohen, F. E. Chiral N-Substituted Glycines Can Form Stable Helical Conformations. *Fold. Des.* **1997**, *2* (6), 369–375. https://doi.org/https://doi.org/10.1016/S1359-0278(97)00051-5.

(34) Wu, C. W.; Sanborn, T. J.; Huang, K.; Zuckermann, R. N.; Barron, A. E. Peptoid Oligomers with α-Chiral, Aromatic Side Chains: Sequence Requirements for the Formation of Stable Peptoid Helices. *J. Am. Chem. Soc.* **2001**, *123* (28), 6778–6784. https://doi.org/10.1021/ja003154n.

(35) Shin, H.-M.; Kang, C.-M.; Yoon, M.-H.; Seo, J. Peptoid Helicity Modulation: Precise Control of Peptoid Secondary Structures via Position-Specific Placement of Chiral Monomers. *Chem. Commun.* **2014**, *50* (34), 4465–4468. https://doi.org/10.1039/C3CC49373C.

(36) Shah, N. H.; Butterfoss, G. L.; Nguyen, K.; Yoo, B.; Bonneau, R.; Rabenstein, D. L.; Kirshenbaum, K. Oligo(N-Aryl Glycines): A New Twist on Structured Peptoids. *J. Am. Chem. Soc.* **2008**, *130* (49), 16622–16632. https://doi.org/10.1021/ja804580n.

(37) Caumes, C.; Roy, O.; Faure, S.; Taillefumier, C. The Click Triazolium Peptoid Side Chain: A Strong Cis-Amide Inducer Enabling Chemical Diversity. *J. Am. Chem. Soc.* **2012**, *134* (23), 9553–9556. https://doi.org/10.1021/ja302342h.

(38) Gorske, B. C.; Bastian, B. L.; Geske, G. D.; Blackwell, H. E. Local and Tunable N→π* Interactions Regulate Amide Isomerism in the Peptoid Backbone. *J. Am. Chem. Soc.* **2007**, *129* (29), 8928–8929. https://doi.org/10.1021/ja071310l.

(39) Gorske, B. C.; Stringer, J. R.; Bastian, B. L.; Fowler, S. A.; Blackwell, H. E. New Strategies for the Design of Folded Peptoids Revealed by a Survey of Noncovalent Interactions in Model Systems. *J. Am. Chem. Soc.* **2009**, *131* (45), 16555–16567. https://doi.org/10.1021/ja907184g.

(40) Zborovsky, L.; Smolyakova, A.; Baskin, M.; Maayan, G. A Pure Polyproline Type I-like Peptoid Helix by Metal Coordination. *Chemistry – A European Journal* **2018**, *24* (5), 1159–1167. https://doi.org/https://doi.org/10.1002/chem.201704497.

(41) Lee, B.-C.; Zuckermann, R. N.; Dill, K. A. Folding a Nonbiological Polymer into a Compact Multihelical Structure. *J. Am. Chem. Soc.* **2005**, *127* (31), 10999–11009. https://doi.org/10.1021/ja0514904.

(42) Pfeiffer, C. T.; Schafmeister, C. E. Solid Phase Synthesis of a Functionalized Bis-Peptide Using “Safety Catch” Methodology. *JoVE* **2012**, No. 63, e4112. https://doi.org/doi:10.3791/4112.

(43) Insuasty Cepeda, D. S.; Pineda Castañeda, H. M.; Rodríguez Mayor, A. V.; García Castañeda, J. E.; Maldonado Villamil, M.; Fierro Medina, R.; Rivera Monroy, Z. J. Synthetic Peptide Purification via Solid-Phase Extraction with Gradient Elution: A Simple, Economical, Fast, and Efficient Methodology. *Molecules* **2019**, *24* (7). https://doi.org/10.3390/molecules24071215.

(44) Duez, Q.; Chirot, F.; Liénard, R.; Josse, T.; Choi, C.; Coulembier, O.; Dugourd, P.; Cornil, J.; Gerbaux, P.; De Winter, J. Polymers for Traveling Wave Ion Mobility Spectrometry Calibration. *J. Am. Soc. Mass Spectrom.* **2017**, *28* (11), 2483–2491. https://doi.org/10.1007/s13361-017-1762-4.

(45) Davies, A. K.; McKellar, J. F.; Phillips, G. O.; Reid, A. G. Photochemical Oxidation of Tetracycline in Aqueous Solution. *J. Chem. Soc., Perkin Trans. 2* **1979**, No. 3, 369–375. https://doi.org/10.1039/P29790000369.

(46) Halin, E.; Hoyas, S.; Lemaur, V.; De Winter, J.; Laurent, S.; Cornil, J.; Roithová, J.; Gerbaux, P. Side-Chain Loss Reactions of Collisionally Activated Protonated Peptoids: A Mechanistic Insight. *Int. J. Mass Spectrom.* **2019**, *435*, 217–226. https://doi.org/https://doi.org/10.1016/j.ijms.2018.10.032.

(47) Kamel, A. M.; Fouda, H. G.; Brown, P. R.; Munson, B. Mass Spectral Characterization of Tetracyclines by Electrospray Ionization, H/D Exchange, and Multiple Stage Mass Spectrometry. *J. Am. Soc. Mass Spectrom.* **2002**, *13* (5), 543–557. https://doi.org/10.1016/S1044-0305(02)00356-2.

(48) Groignet, L.; Dellemme, D.; Duez, Q.; Fizazi, A.; Colet, J.-M.; Brocorens, P.; Surin, M.; Gerbaux, P.; De Winter, J. Impact of Post-Translational Succination on Small Ubiquitin-Like Modifier 1 Structure: A Dual Approach Combining Gas Phase and Solution Studies. *ACS Pharmacol. Transl. Sci.* **2025**, *8* (8), 2683–2693. https://doi.org/10.1021/acsptsci.5c00259.

(49) Fowler, S. A.; Blackwell, H. E. Structure–Function Relationships in Peptoids: Recent Advances toward Deciphering the Structural Requirements for Biological Function. *Org. Biomol. Chem.* **2009**, *7* (8), 1508–1524. https://doi.org/10.1039/B817980H.